Neuron 49, 143–155, January 5, 2006 ©2006 Elsevier Inc. DOI 10.1016/j.neuron.2005.10.037

# Place-Selective Firing of CA1 Pyramidal Cells during Sharp Wave/Ripple Network Patterns in Exploratory Behavior

**Joseph O'Neill,[1] Timothy Senior,[1] and Jozsef Csicsvari[1,*]**
[1] MRC Anatomical Neuropharmacology Unit
Department of Pharmacology
University of Oxford
Mansfield Road
Oxford OX1 3TH
United Kingdom

## Summary

**We observed sharp wave/ripples (SWR) during exploration within brief (<2.4 s) interruptions of or during theta oscillations. CA1 network responses of SWRs occurring during exploration (eSWR) and SWRs detected in waking immobility or sleep were similar. However, neuronal activity during eSWR was location dependent, and eSWR-related firing was stronger inside the place field than outside. The eSPW-related firing increase was stronger than the baseline increase inside compared to outside, suggesting a "supralinear" summation of eSWR and place-selective inputs. Pairs of cells with similar place fields and/or correlated firing during exploration showed stronger coactivation during eSWRs and subsequent sleep-SWRs. Sequential activation of place cells was not required for the reactivation of waking co-firing patterns; cell pairs with symmetrical cross-correlations still showed reactivated waking co-firing patterns during sleep-SWRs. We suggest that place-selective firing during eSWRs facilitates initial associations between cells with similar place fields that enable place-related ensemble patterns to recur during subsequent sleep-SWRs.**

## Introduction

It is believed that the hippocampus is involved in the consolidation of certain types of memories, by temporarily storing labile memory traces of waking experience that are subsequently reactivated and transferred back to other cortical areas (Squire and Zola-Morgan, 1991; Buzsaki, 1989). The initial memory storage and reactivation/consolidation phases are believed to occur in separate behavioral states; labile memories are formed during waking exploration, while reactivation occurs primarily during immobility, consummatory behaviors, and sleep (Buzsaki, 1989; Wilson and McNaughton, 1994). These behavioral states correspond with characteristically different physiological network states and associated network patterns in the hippocampus.

During exploratory behavior (locomotor activity) and rapid eye movement (REM) sleep, the rhythmic theta (6–12 Hz) oscillation is the dominant network activity pattern in the rodent hippocampus (Vanderwolf, 1969; cf. Buzsaki, 2002). In parallel with waking theta oscillations, hippocampal principal cells fire in a location-dependent manner (O'Keefe and Dostrovsky, 1971; O'Keefe and Nadel, 1978). In the absence of theta oscillations (e.g., waking immobility, slow wave sleep), irregularly occurring sharp waves are the most dominant network pattern observed in CA1 stratum radiatum (Buzsaki et al., 1983). Both CA3 and CA1 pyramidal cells fire synchronously during sharp waves (Buzsaki, 1986; Csicsvari et al., 2000), and the strong excitatory input from the CA3 region triggers short-lived fast (140–200 Hz) oscillatory patterns ("ripples") in the CA1 region (O'Keefe and Nadel, 1978; Suzuki and Smith, 1988; Buzsaki et al., 1992; Ylinen et al., 1995; Draguhn et al., 1998; Csicsvari et al., 1999a, 1999b; Traub and Bibbig, 2000).

The hypothesis that the reactivation-consolidation process takes place in the hippocampus is supported by several studies showing that neuronal activity patterns observed during waking exploration recur in subsequent sleep. It has been shown that cells that fire together during exploration also do so in sleep (Kudrimoti et al., 1999; Hirase et al., 2001). Furthermore, cells with overlapping place fields showed correlated firing during sleep, indicating that place-related activity is reactivated during sleep (Wilson and McNaughton, 1994). Finally, it has been demonstrated that sequential firing of place cells recurs during sleep, but only after they have been repeatedly activated in the same order during behavior, e.g., on linear tracks or circular mazes (Skaggs and McNaughton, 1996; Louie and Wilson, 2001; Lee and Wilson, 2002, 2004).

Because CA3-CA1 neuronal activity during sleep occurs frequently in synchronous bursts associated with SWRs, it has been suggested that reactivation of neuronal assemblies is confined mostly to SWRs. Furthermore, it has been hypothesized that the key pattern for consolidation of learned information is SWRs, not sleep per se (Buzsaki, 1989, 1996; Nadasdy et al., 1999; Kudrimoti et al., 1999). Indeed, there are indications that organized ensembles of CA3 and CA1 cells fire in SWRs (Nadasdy et al., 1999; Kudrimoti et al., 1999; Csicsvari et al., 2000; Lee and Wilson, 2002, 2004), some correlated with waking neuronal patterns (Kudrimoti et al., 1999).

Although the reactivation of waking activity patterns has been confirmed by many studies, the mechanism underlying reactivation has not yet been resolved. In particular, it is not known how new waking firing patterns of cell assemblies are incorporated into existing SWR patterns. Several studies proposed that plasticity occurs between sequentially activated place cells during waking theta oscillations, e.g., place cells in linear track experiments (Skaggs et al., 1996; Mehta et al., 2000, 2002; Ekstrom et al., 2001). This would enable spike-timing-dependent plasticity (STDP) (Markram et al., 1997; Bi and Poo, 1998), which may facilitate the reactivation of firing sequences. However, pairing neuronal firing with the SWR itself can facilitate assembly formation. The time course of SWRs is optimal for synaptic plasticity (Magee and Johnston, 1997). Furthermore, plastic changes during SWRs have been demonstrated by stimulating CA1 pyramidal cells during SWRs,

*Correspondence: jozsef.csicsvari@pharm.ox.ac.uk

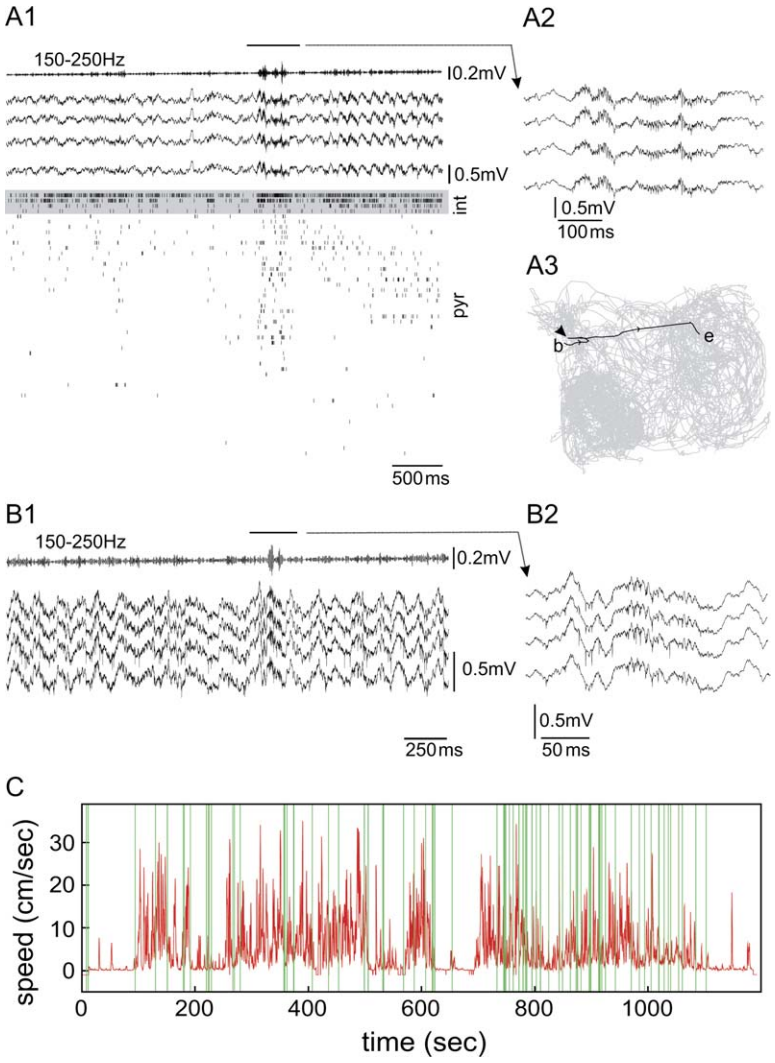


Figure 1. SWRs Observed in Spatial Exploratory Periods

(A) Local field and network response during SWR pattern observed in a brief (~2 s) interruption of the theta oscillation. Top trace: band-pass filtered (150–250 Hz) signal of a tetrode channel shown below. Bottom traces: wide-band (1 Hz to 5 kHz) traces recorded from a wire tetrode. Raster plot: spike timing of simultaneously recorded CA1 pyramidal cells (n = 46) and interneurons (n = 4). The vertical lines indicate the action potential times of cells. int, CA1 pyramidal layer interneurons; pyr, CA1 pyramidal cells. The top horizontal interval bar marks the time period shown in (A2).

(A3) The movement path of the animal. The black line, movement path for time period in (A1); gray tracks, movement path for the whole recording session. b, beginning of the path; filled arrow, the location of the animal when the eSWR occurred; e, end of the path.

(B1) and (B2) An eSWR that was observed "nested" on a theta oscillatory wave. Band pass-filtered (150–250 Hz) and wide-band (1 Hz to 5 Khz) recordings are shown from a single tetrode. The horizontal interval bar marks the time period shown in (B1).

(C) The instantaneous speed of the animal is plotted together with the times when eSWRs (vertical green lines) are detected in a 20 min exploration session. No food reward was applied in this session.

which caused their firing to be potentiated with subsequent SWRs (King et al., 1999).

Here, we report that theta oscillations are not continuous during exploration but are irregularly interrupted by SWR patterns. We hypothesized that these exploration-associated network burst patterns (i.e., eSWRs) provide a mechanism by which cell assemblies that encode the same part of the environment, and thus fire together in space, are incorporated into existing SWR assemblies. Once incorporated into the SWR, the same cell assembly can be reactivated during subsequent SWRs during immobility or sleep. Therefore, we suggest that eSWRs have a role in plastic processes enabling reactivation. To test this hypothesis, we examined whether the background network synchronization associated with SWRs overlaps with place-selective firing, ensuring similar conditions to those shown to cause the potentiation of SWR firing in the King et al. (1999) study. In addition, we tested whether such place-selective assemblies are reactivated during sleep SWRs. Finally, to test whether STDP alone can explain reactivation during SWRs, we checked whether firing sequences or merely conjoint firing patterns (without sequential bias) are reactivated during SWRs.

## Results

We recorded local field potential (LFP) and multiple-unit activity in the CA1 region during spontaneous and food-reinforced spatial exploration, waking-immobility, and sleep. Waking sessions were split into immobility and exploratory periods by monitoring both the movement speed of the animal and theta/delta power ratio (see Experimental Procedures). Exploratory periods included brief (<2.4 s; as set by the theta detection procedure) periods of immobility and reduced theta/delta power, whereas longer periods were considered waking immobility.

SWR events containing several individual oscillatory ripple waves (e.g., see Figure 2A) were detected by calculating power in the ripple band (150–250 Hz; see Experimental Procedures). In addition to SWRs observed during slow wave sleep (sSWRs) and waking immobility (iSWRs), we have observed SWRs during exploratory periods. The SWRs during exploratory periods (i.e., eSWRs) occurred when theta oscillations were briefly (<2.4 s) interrupted and the speed of the animal was transiently reduced (Figure 1A and Figure S1). More rarely, eSWRs were "nested" within theta oscillations

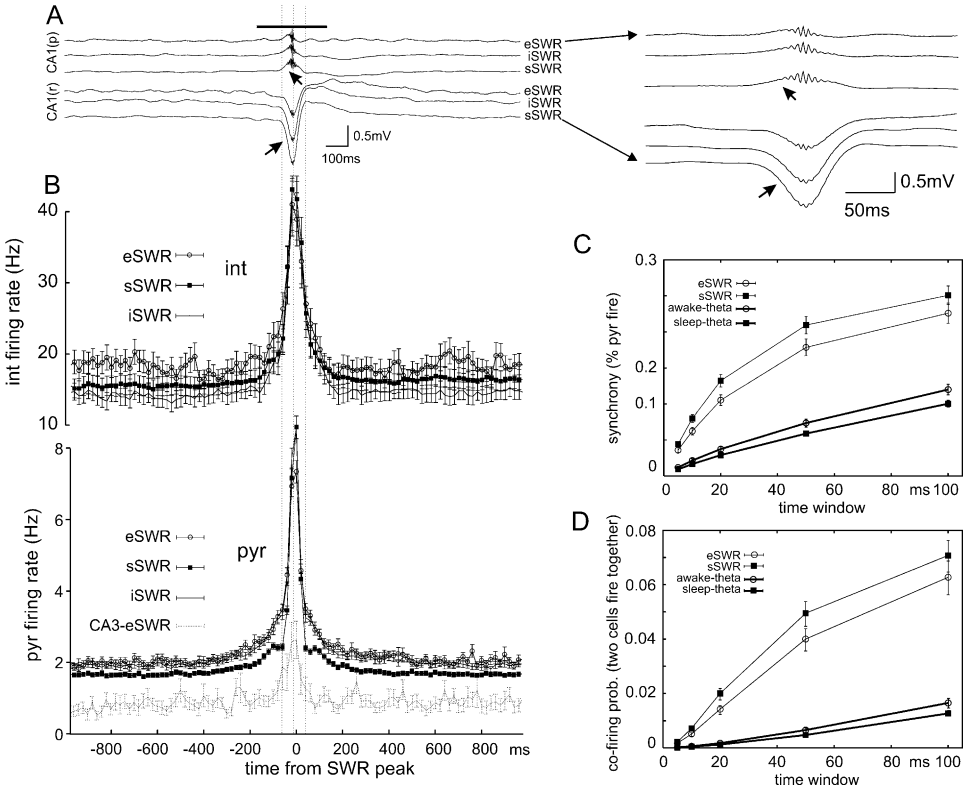


Figure 2. SWR Network Responses during Different Behavioral States

(A) Average local field potential patterns of the SWR network pattern recorded from two electrodes, one electrode positioned in the CA1 pyramidal layer [CA1(p)] and the other in the CA1 stratum radiatum [CA1(r)]. Field responses were averaged at positive ripple peak times that were within 2 ms from the SWR peaks (eSWR, n = 1069; iSWR, n = 2185; sSWR, n = 4477). Sharp waves (see filled arrows) were negative in the stratum radiatum and positive in the CA1 pyramidal layer. Note the reduced sharp wave amplitudes in the stratum radiatum during eSWRs. The horizontal interval bar (left panel) marks the time period that is shown on the right panel. Vertical dotted lines mark the beginning peak and end of the sharp waves recorded in the stratum radiatum.

(B) Mean (±SE) firing rate histograms of CA1 interneurons (int, n = 102), CA1 pyramidal cells (pyr, n = 652) during e/i/sSWR and CA3 pyramidal cells (n = 81) during eSWRs (CA3-eSWR). CA3 pyramidal responses were similar during sSWRs and iSWRs as well (data not shown). Histograms were aligned to the left panel of the field responses in (A). Firing rates were measured in 20 ms bins in reference to SWR peaks.

(C) Synchrony and (D) co-firing probability of CA1 pyramidal cells during SWR and theta oscillations as a function of time window size. Network synchrony was defined as the average percentage of pyramidal cells that fired together in the time windows, whereas the co-firing probability of cell pairs referred to the probability that both cells fire together in the time window. Time windows were centered on the peaks of SWR (peak of ripple-band power) and the negative peaks of theta oscillations. Note the 2- to 4-fold higher synchrony and 4- to 12-fold stronger co-firing during SWR as compared to theta oscillatory epochs (eSWR, waking-theta, n = 20; sSWR, sleep REM, n = 17).

(Figure 1B). SWRs have been associated with consummatory behavior and have been observed following the consumption of water reward in the wheel-running apparatus (Buzsaki et al., 1983; Czurko et al., 1999). If eating food has a similar effect, some of the eSWRs that we observed may have been related to consumption of the food reward. However, they occurred also in sessions when food reward was not provided (example: Figure 1C). We observed eSWRs in all adult (3–8 months) rats and the single young (2.5 month) Sprauge-Dawley rat (Figure S2). In the young rat, we did not observe spike-and-wave or high-voltage spindle events in cortical LFPs, confirming that such events are not required to trigger eSWRs.

As is the case during i/sSWRs, negative sharp waves are observed in the CA1 stratum radiatum during eSWRs (Figure 2A), whereas sharp waves were positive in the CA1 pyramidal layer in all three conditions. Sharp wave amplitudes in the stratum radiatum were 30%–60% smaller during eSWRs as compared to sSWRs (n = 9 sessions). The duration of the detected SWR events was similar across the three different conditions (eSWR, 57.8 ± 2.3 ms; iSWR, 61.3 ± 1.9 ms; sSWR, 61.8 ± 1.8 ms; all n values = 16; $p > 0.3$ ANOVA). The average wavelength of the detected ripple waves was shortest during eSWRs and longest in sSWRs (eSWR, 5.07 ± 0.04 ms; iSWR, 5.17 ± 0.05 ms; sSWR, 5.24 ± 0.05 ms; all n values = 16; $p < 0.05$ ANOVA). eSWRs occurred significantly less frequently than iSWRs or sSWRs (eSWR, 0.08 ± 0.01 Hz; iSWR, 0.43 ± 0.05 Hz; sSWR, 0.45 ± 0.05 Hz; all n values = 16 sessions; $p < 0.001$ ANOVA).

### SWRs in Different Behavioral States

To compare the network activation patterns of SWRs in different states, the mean SWR firing histograms of CA1 pyramidal cells and CA1 interneurons were calculated (see Figure 2B) by measuring the mean firing rate of cells relative to SWR peak times (i.e., peak of ripple power within the SWR event, see Experimental Procedures). Overall, the activation patterns of CA1 pyramidal

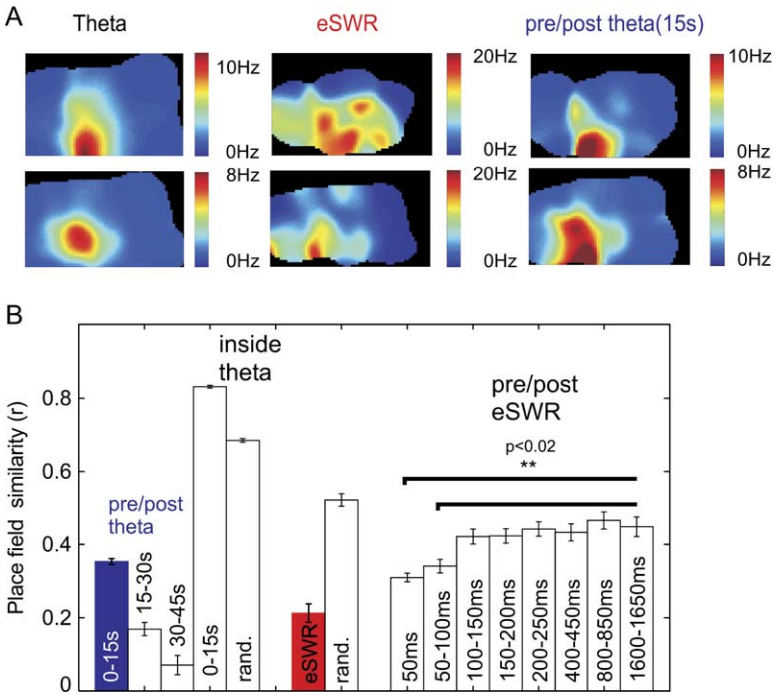


Figure 3. Place Rate-Maps in Waking Theta, eSWRs, and Waking Non-Theta Epochs

(A) Two examples of place rate-maps calculated during theta oscillations, eSWR and in 15 s windows surrounding (i.e., immediately preceding and following) theta oscillations.

(B) Change of place rate-map similarity during eSWRs and waking non-theta epochs. Place rate-maps were cross-correlated and the correlation coefficient was calculated in order to compare them. The mean correlation coefficients are shown (±SE). Place rate-maps acquired during theta oscillations were compared to those during non-theta epochs in 0–15 s, 15–30 s, and 30–45 s epochs surrounding theta oscillations. Further comparisons were made between theta rate-maps and rate-maps during eSWRs, the 100 ms windows centered around eSWRs and in adjacent 50 ms time windows on both side of eSWRs. rand, "bootstrapped" place rate-maps were calculated from randomly selected spikes that occurred during theta oscillation (excluding eSWRs) using the same number of sampled spikes as recorded during eSWRs or in the 15 s windows surrounding the theta border.

cells and CA1 pyramidal-layer interneurons were similar across the three conditions (Figure 2B). However, the baseline firing rate of CA1 pyramidal cells 1–0.4 s prior to the onset of SWRs was significantly higher during waking theta than during slow wave sleep ($p < 0.005$, ANOVA). This is in agreement with the finding that the mean firing rate of CA1 pyramidal cells is higher during theta oscillations as compared to non-SWR slow wave sleep (Csicsvari et al., 1999a).

In the analyses above, we measured the timing of cells relative to the SWR event itself, but not in relation to individual ripple waves. In order to examine the oscillatory firing of cells to ripple oscillations, unit firing was related to the times of ripple oscillatory waves, and the mean ripple phase of unit firing was calculated in the three conditions. Only cells with significant phase locking to ripples ($p < 0.05$, Rayleigh test) were considered. Across all three states, the mean ripple phase of pyramidal cells (eSWR, 28.6° ± 10.7°, n = 298; iSWR, 33.1° ± 8.8°, n = 476; sSWR, 27.3° ± 6.4°, n = 472) and interneurons (eSWR, 82.2° ± 28.5°, n = 76; iSWR, 82.7° ± 20.5°, n = 89; sSWR, 75.7° ± 16.4°, n = 83) was not significantly different between the three conditions (all p values > 0.2, Watson-Williams circular test).

To quantify network participation in eSWRs and sSWRs, we calculated the network synchrony of pyramidal cells during theta oscillations and SWRs both in active waking and sleep. Network synchrony was defined as the percentage of pyramidal cells that fire together in 5–100 ms time windows. During both sSWRs and eSWRs, the network synchrony of pyramidal cells was higher than during theta oscillations (Figure 2C).

### Place Fields during eSWRs and Waking Non-Theta Periods

Because theta activity was disrupted and/or transiently desynchronized during eSWRs, place-related firing of cells may be altered during eSWRs. Thus, place-firing rate-maps (place rate-map) calculated during waking theta oscillations were compared to those calculated during eSWRs (Figure 3A). Pearson's correlation coefficient was used to quantify the similarity between place rate-maps. Place cells fired fewer action potentials during eSWRs than during theta activity, causing an increase in sampling error. Therefore, we randomly selected the same number of action potentials from theta epochs as the total recorded during eSWRs. Nevertheless, even this "bootstrapped" theta place rate-map correlation was significantly larger ($p < 0.001$, paired t test, n = 182) than that of eSWRs.

Next we examined place-related firing in the transition between theta and eSWRs. We calculated place rate-maps based on pairs of 50 ms time windows centered on (but at increasing distances from) the peak of eSWRs and compared them to the theta place rate-maps. Only the window pairs covering ±0–50 ms and ±50–100 ms from the eSWR peak showed a significant difference to subsequent window pairs (Figure 3B, $p < 0.02$, ANOVA with Fisher's LSD post hoc). This suggests that place encoding returns to normal within 100–150 ms from the eSWR peak.

The network state and consequently place-selective firing that occurs immediately before and after theta oscillations may be similar to that surrounding eSWRs, where theta activity is briefly interrupted. Thus, we examined place rate-maps of pyramidal cells in time periods before and after periods of theta oscillation. First, place rate-maps in time periods adjacent to the theta periods were compared to the theta place rate-maps. Place rate-map similarity in 15 s windows surrounding theta epochs showed a significant reduction as compared to "bootstrapped" place rate-maps or place rate-maps measured in 15 s windows inside theta periods, adjacent to theta/non-theta borders (all p values < 0.001,

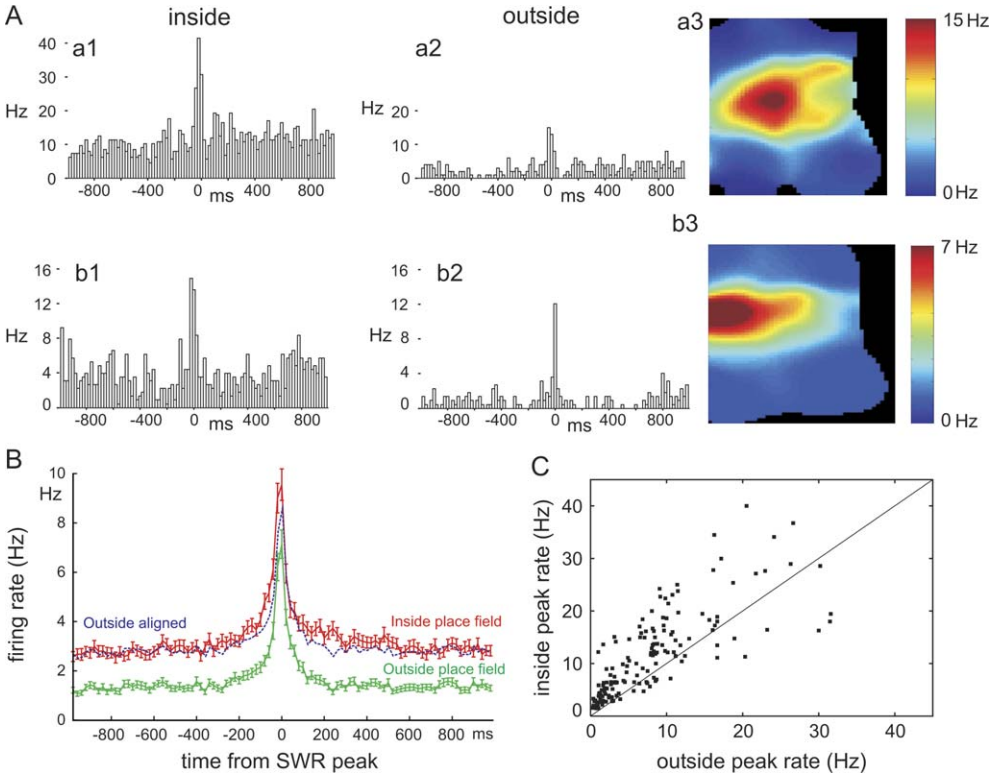


Figure 4. eSWR Firing of Pyramidal Cells Inside and Outside Their Place Fields

(A) Example pyramidal cell firing response inside and outside their place fields during eSWRs. eSWR firing of two place cells (from different animals) inside and outside their place field is shown in (Aa1)–(Aa3) and (Ab1)–(Ab3). The first cell (Aa1–Aa3) had larger eSWR peak firing inside the place field. The second cell (Ab1–A3) also showed widened eSWR firing inside the place field. The eSWR firings were calculated separately for locations where the place rate-map was above or below a threshold ([Aa1–Aa3], 5 Hz; [Ab1–Ab3], 2 Hz). Place rate-maps were calculated during waking theta oscillation.

(B) eSWR network response of spatially active pyramidal cells and pyramidal cells that fire outside their place field. The firing rate threshold was set automatically by measuring mean, baseline firing rate in 50% of the place rate-map bins with the lowest firing rate. The threshold for inside the place field was set to two times the baseline rate, and bins with less than baseline rate were considered as outside the place field. n = 159 pyramidal cell responses were averaged (±SE). Dotted blue line, outside SWR curve, realigned to the same baseline as the inside SWR curve. Note the reduced peak of the realigned curve relative to the inside the SWR curve.

(C) Scatter plot of the peak eSWR firing rate of individual place cells inside and outside the place field.

t test, all n values > 1800). Next, place rate-maps were calculated in 15 s time windows further away (15 s and 30 s), where we observed an additional, significant reduction in place rate-map similarity (all p values < 0.002, t test, all n values > 320) and, thus, a gradual reduction of place encoding over time from the theta borders.

### SWR-Associated Firing Inside/Outside Place Field

Place rate-maps measured 100–150 ms from eSWR peaks were similar to those measured further away from SWRs (e.g., 1.6 s away) when place-selective activity is expected to be normal. This suggests that place-selective activity is present just before the onset of eSWR and, therefore, eSWR network bursts may overlap with ongoing place-selective activity. In this scenario, both place-selective and eSWR inputs may facilitate the firing of place cells, these inputs potentially summating. To test this hypothesis, we calculated the eSWR firing rate histogram of CA1 place cells separately for eSWRs that occur inside and outside the place field. Both the baseline and the peak eSWR firing rates were significantly higher inside the place field (Figure 4B) as compared to outside; baseline rate, 2.93 ± 0.18 Hz versus 1.12 ± 0.08 Hz; peak rate, 11.73 ± 0.71 Hz versus 8.28 ± 0.68 Hz (all p values < 0.001, paired t test n = 159). Baseline firing rate differences confirm that place-selective firing exists immediately prior to eSWRs, whereas the similar increased eSWR firing inside the place field shows the joint facilitation of SWR and place-selective inputs. A higher SWR firing inside the place field was observed for 85% of the cells (Figure 4C).

Next, we examined whether eSWR firing rate from outside to inside the place field increased as much as the baseline increase. We detected a stronger increase in eSWRs firing rate than the baseline increase when the outside eSWR histogram was aligned to the same baseline level as the inside histogram (see blue dotted line in Figure 4B). In addition, the difference between eSWR peak firing rates was significantly higher than the difference in the baseline rates ($p < 0.005$, paired t test, n = 159). These observations showed that the increased eSWR firing inside the place field increased over and above that caused by the increase of baseline firing.

iSWR firing responses that occurred in the 15 s periods surrounding theta oscillations were also compared

inside and outside the place field to determine whether those iSWRs detected close to theta periods show place-selective responses. Similar to eSWRs, both the baseline and peak firing rates increased significantly: baseline, 2.73 ± 0.1 Hz versus 2.01 ± 0.07 Hz; peak, 13.14 ± 0.51 Hz versus 12.18 ± 0.34 Hz (all p values < 0.02, paired t test, n = 296). However, the differences between the peak SWR rates (inside versus outside) were more than 3-fold smaller than for eSWRs. Furthermore, iSWRs occurring in 15–30 s time windows surrounding theta oscillations did not show significant differences in their baseline or peak rate inside versus outside the place field (all p values > 0.89, paired t test, n = 107). Thus, place-selective firing was preserved for iSWRs that occurred 15 s before or after theta oscillations, but not for iSWRs that occurred further outside theta periods.

To establish whether CA3 input contributes to the place-selective firing rate increase of CA1 pyramidal cells during eSWR, we compared the eSWR firing of CA3 pyramidal cells inside and outside their place fields. Similar to CA1 pyramidal cells, CA3 pyramidal cells also showed place-selective firing rate increases during eSWRs. Both their peak and baseline firing rate was significantly higher inside the place field than outside; baseline, 1.59 ± 0.25 Hz versus 0.42 ± 0.08 Hz; peak, 5.09 ± 1.4 Hz versus 2.18 ± 0.56 Hz (all p values < 0.01, paired t test, n = 18).

### SWR Firing at Different Baseline Firing Rates

To test independently whether the increased firing inside the place field corresponds with an increased eSWR peak firing, we examined the eSWR peak firing rates that occurred at different baseline rates. Furthermore, this relationship between baseline/peak firing rates can be measured during sleep (i.e., for sSWRs) when place-selective activity is not present. Therefore, if indeed the increased eSWR peaks inside the place field are the result of the summation of place-selective and eSWR inputs, it is expected that baseline-against-peak function of eSWRs will be different to that of sSWRs.

The number of action potentials in 1 s windows centered on SWR peaks was used to differentiate SWRs at different cell activity levels. Separate firing rate histograms were calculated for SWRs for different action potential numbers, and both the baseline firing (−1 to −0.75s before SWR) and peak firing (−100 to 100 ms) of these histograms were determined. The peak rates monotonically increased as a function of the baseline rate (Figure 5B), confirming that inside the place field, where the baseline rate is higher, the eSWR peak rate is expected to be higher than outside. There was, however, a nonlinear relationship between baseline and peak rate; the rate of increase was reduced at higher baseline values. Furthermore, this saturation of the baseline peak curve was more pronounced for eSWRs, which are accompanied by higher firing rates when place-selective firing occurs.

In addition to confirming the place-selective firing during eSWRs, baseline peak histograms showed also that the eSWR peak firing inside the place field (relative to outside) increased more than predicted by the baseline increase. If the eSWR peak firing rate increase equals the baseline increase, a change in baseline rate should

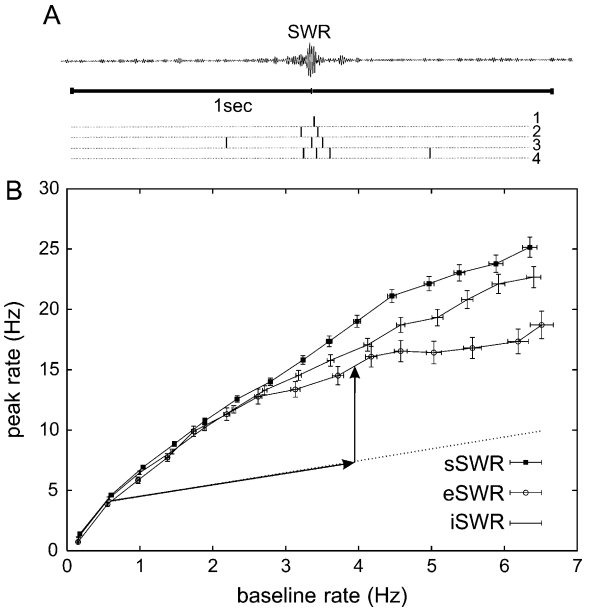


Figure 5. Behavioral State-Dependent Nonlinearity of SWR Responses

(A) Explanation of the method to test the correlation between baseline and peak SWR-firing rate. One second windows were centered on SWR peaks, and firing responses were sorted according to the number of action potentials.

(B) SWR peak firing rate as a function of the baseline firing rate for eSWR, sSWR, and iSWR. Note that an increase in the number of spikes in the 1 s time windows resulted in both increased mean baseline and peak firing rates. Baseline and peak rates of individual cells were measured at [−1 s; −0.75 s] and [−100 ms; 100 ms] bins, respectively. The mean (±SE) baseline/peak response (eSWR, n = 118; iSWR, n = 291; sSWR, n = 389) was plotted for different network states. Dotted line, a line parallel with y = x curve intercepting the eSWR curve at x = 0.5 Hz. Arrows demonstrate a firing rate change when the baseline rate of a cell changes from 0.5 Hz to 4 Hz outside versus inside the place field. eSWR curve is well above the dotted line that would correspond with the sum of eSWR-response outside the place field and the baseline increase.

be accompanied by an equal change in peak rate and, thus, a line parallel with x = y (and intercepting the eSWR curve at the baseline rate) would determine the eSWR peak firing (see Figure 5B). The first derivative of the eSWR curves (as well as the other curves) was >1 at baseline rates <4 Hz. Thus, if the baseline firing rate outside the place field was <4 Hz, the eSWR peak firing rate increase inside will be higher than the baseline increase.

### Stronger Joint-Firing of Place Cells with Overlapping Place Fields during SWRs

In order to test the reactivation of patterns during SWRs, the average cross-correlograms of cell pairs with similar or different place fields were calculated during eSWRs and theta oscillations (Figure 6). The average cross-correlations of cell pairs with overlapping place fields showed stronger cross-correlograms than cells with nonoverlapping place fields. The correlation probability was almost three times stronger during eSWRs than it was during theta activity. Furthermore, in sleep periods following exploration, the cross-correlation of cell pairs with similar place fields was stronger than that of nonoverlapping place field pairs (Figure 6), whereas the

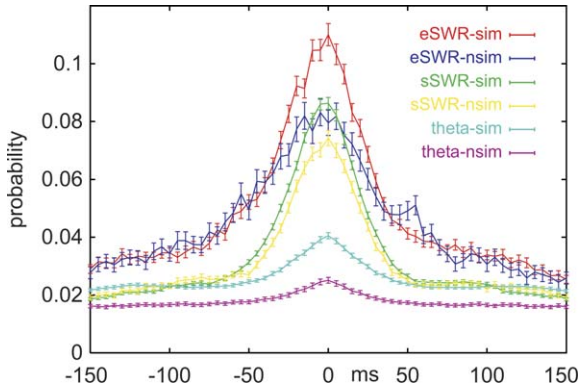


Figure 6. Increased Cross-Correlation of Place Cells with Similar Place Fields during Theta, eSWR, and Post-sSWRs

Mean cross-correlations of pyramidal cell pairs (±SE) with similar place fields ($r > 0.4$, n = 851 pairs) and nonoverlapping fields ($r < -0.4$, n = 331 pairs) are plotted. The same cell-pairs were calculated for theta, eSWR, and post-sSWR. sim, cell pairs with similar place field; nsim, cell pairs with nonoverlapping place field.

same correlations were similar in pre-sleep periods (data not shown; $p > 0.72$, t test measured as the average of bins [−10 ms;10 ms]).

In addition to the cross-correlations used above, we also used the Pearson's correlation coefficient of the instantaneous firing rates (i.e., spike counts in bins) to show the reactivation of waking ensemble patterns during sleep (Wilson and McNaughton, 1994; Kudrimoti et al., 1999). Because this correlation measures joint firing rate changes, it is better suited to show reactivation than correlation histograms. We refer to this correlation as the instantaneous firing rate correlation (IFRC). Cells with high IFRCs during theta periods also showed significantly stronger IFRCs during eSWRs and sSWRs following exploration (post-sSWR) than cells with low IFRCs (all p values < 0.001, t test; Figure 7A). A similar relationship was observed for post-sSWRs when high and low IFRC pairs were selected during eSWRs (Figure 7A). Furthermore, this difference was smaller in sSWRs prior to exploration (pre-sSWR) when either theta or eSWR correlations were used as reference. Second, a significant regression is observed when theta-IFRCs were compared to eSWR or post-sSWR IFRCs and when eSWRs and post-sSWRs IFRCs were compared (all p values < 0.001, Figure 7B).

Next, we tested whether the joint firing of cells during SWRs is due to spatially selective or location-independent assembly firings. Therefore, we tested whether there is a direct relationship between place field similarity and IFRCs during eSWRs and sSWRs. Similar to the previous analysis with theta correlations, cell pairs with similar place fields showed significantly higher IFRC during eSWR and post-sSWRs, and this difference was smaller in pre-sSWR (Figure 7C). In addition, there was a significant regression between place-field similarity and IFRCs for eSWR and post-sSWR (all p values < 0.001); this was reduced for pre-sSWRs (Figure 7D).

### Reactivation of Co-Firing Patterns in the Absence of Temporal Sequences

Here, we tested whether reactivation of firing sequences can be observed in our data set. We tested whether cell pairs that show preferential order in their firing during exploration maintain a similar relationship during post-sSWRs or eSWRs. The asymmetry in the cross-correlation histograms of cell pairs was calculated both in exploration and during e/sSWRs, and a regression was performed. A significant regression was observed between the cross-correlation asymmetries of theta with eSWR and theta with post-sSWR, as well as eSWR with post-sSWR (all p values < 0.001). Regressions with pre-sSWR were not significant (all p values > 0.1). However, the correlation coefficients were small in all cases ($r < 0.1$, Figure 7E). One possible reason for the small correlation coefficients was that most of our experiments were performed in open-field environments. Therefore, most cell pairs showed neither a strong bias in the temporal order of their firings during exploration nor a preserved cross-correlation asymmetry during sleep.

Overall, the stronger regression between IFRCs as compared to cross-correlation asymmetry suggests that not all cell pairs that showed reactivation in their IFRCs (i.e., co-firing) maintained a similar relationship in their cross-correlation asymmetry. Therefore, the sequential firing of cells may not be required for waking co-firing patterns to be reactivated in sleep. To confirm this, we tested whether significant regression of the IFRCs is observed for cell pairs that had nearly symmetrical cross-correlations and did not show significant regression of cross-correlation asymmetries. Cell pairs with less than 2% (i.e., 0.02) cross-correlation asymmetry had no significant regression in their cross-correlation asymmetry between theta-eSWRs, theta-pre/post sSWRs, or eSWR-pre/post sSWRs (all p values > 0.2), whereas their IFRC regressions remained significant for the same conditions (Figure 7F, all p values < 0.001). Thus, we confirmed that cell pairs that do not show reactivated sequence bias, and that have nearly symmetrical cross-correlation histograms, still show a recurrence of the waking co-firing patterns during sleep.

### Ongoing Changes of SWR Co-Firing Patterns during Exploration and Sleep

SWR co-firing patterns may gradually change during the course of waking and sleep sessions in relation to the co-firing patterns of waking theta activity, in which case the regression coefficient between theta-SWR IFRCs is expected to change. To assess the variability of the regression coefficient, a regression was performed session by session. Regression coefficients calculated within a session compared the similarity of the co-firing matrices (as constructed by all possible combinations of cell pairs) of the recorded cell assembly, and therefore it estimated the accuracy of replay for the recorded cell assembly. First, we compared the mean assembly correlation coefficients for theta-eSWRs, theta-iSWR, and theta-post sSWRs correlations; the theta-post sSWRs correlation coefficient was significantly larger than that of theta-eSWRs (Figure 8A, $p < 0.05$, ANOVA with Fisher's LSD post hoc). This result suggests that SWR co-firing patterns may improve gradually to represent theta patterns (either during waking or even during sleep). To compare whether changes of the regression coefficient may occur during waking exploration or sleep, a regression was performed between waking theta IFRCs and SWR (eSWRs, iSWRs, and post-sSWRs) IFRCs,

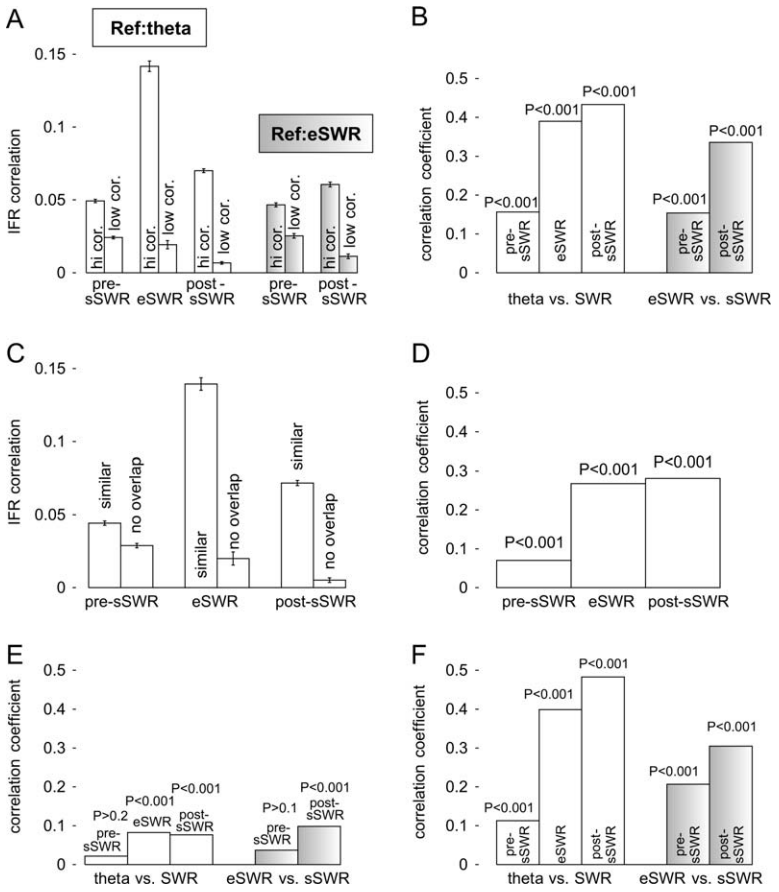


Figure 7. Preserved Cross-Correlation Asymmetry and Co-Firing of Place Cells with Similar Place Fields during eSWR and Post-sSWR

(A) Cells with a strong IFRC during theta or eSWR epochs (i.e., ref: theta and ref: eSWR) also show stronger IFRCs in eSWR and post-sSWR than those with a weak correlation, but a reduced increase in pre-sSWR. Cell pairs were sorted according to their reference (theta or eSWR) IFRC (hi > 0.02; low < 0.01), and the mean (±SE) IFRCs in eSWR and sSWRs were calculated separately for the "hi" and "low" groups.

(B) The correlation coefficient for the regression between theta-e/sSWR and eSWR-sSWR IFRCs (theta versus pre-sSWR, n = 16073; theta versus eSWR, n = 6763; theta versus post-sSWR, n = 15761; eSWR versus pre-SWR, n = 6591; eSWR versus post-sSWR, n = 6643).

(C) The mean (±SE) IFRC of cells with similar (r > 0.2) and nonoverlapping (r < −0.2) place fields were calculated during eSWR and pre/post-sSWRs. Place cell similarity was measured by the correlation coefficient between place rate-maps. Note the larger IFRC for cell pairs with similar place fields during eSWR and post-sSWRs than those with nonoverlapping fields and the reduction of this difference during pre-sSWR.

(D) The correlation coefficient was measured between place field similarity and IFRC during SWRs (pre-sSWR, n = 13508; eSWR, n = 6261; post-sSWR, n = 13275).

(E) The regression between cross-correlation histogram asymmetries measured during theta versus e/sSWR and eSWR versus sSWR. To measure the asymmetry of the cross-correlation histogram, the total number of action potentials in time bins [0, 100 ms] and [−100, 0 ms] were calculated and the difference divided by the sum of spikes in both intervals. Only cell pairs with overlapping place fields (r > 0.2) were included in the analyses (theta versus pre-sSWR, n = 3681; theta versus eSWR, n = 1790; theta versus post-sSWR, n = 3695; eSWR versus pre-SWR, n = 1736; eSWR versus post-sSWR, n = 1755).

(F) Regression performed on IFRCs for cell pairs with <0.02 cross-correlation asymmetry. All the regressions were significant (all p values < 0.001). Theta versus pre-sSWR, n = 2523; theta versus eSWR, n = 1282; theta versus post-sSWR, n = 2480; eSWR versus pre-SWR, 312; eSWR versus post-sSWR, n = 317.

measured in the beginning and end of individual sessions (either sleep of waking). The mean assembly correlation coefficients calculated in the first and last 10 min of the session were not significantly different for either eSWRs or post-sSWRs (eSWR, p > 0.2, n = 11; post-sSWR, p > 0.1, n = 18, paired t tests). However, theta-iSWR correlation coefficients were significantly larger at the end of the session as compared to the beginning (p < 0.05, paired t test, n = 14). This suggests that iSWRs patterns have an improving relationship with waking co-firing patterns and more closely resemble the waking exploratory patterns toward the end of the waking sessions.

## Discussion

In this paper, we have shown that SWRs are observed during the spatial exploration task. We found that place-selective firing remained in these eSWRs through an increased background level of firing, suggesting that SWR input (originating from the CA3 region) and place-selective activity conjointly facilitate place cell firing during eSWRs. We propose that eSWRs promote the formation of assemblies of cells with similar place fields, thus contributing to plastic processes that enable the replay of waking activity patterns during sleep. We have confirmed that such place-related assembly patterns are reactivated during s/iSWRs; place cells with similar place fields tend to fire together more during subsequent i/sSWRs. We have also shown that sequential activation of cell pairs is not required to observe such a reactivation of waking co-firing patterns during sSWRs, suggesting that STDP is not required for the reactivation of co-firing patterns during SWRs.

Before discussing the hypothesized role of eSWRs to incorporate waking assemblies patterns into existing SWRs patterns, we discuss network events that lead to eSWRs patterns and the assembly coding nature of the reactivated SWR patterns.

### Network Mechanism of eSPWs

Our data showed that, similar to i/sSWRs, CA3 inputs depolarize the dendrites of CA1 pyramidal cells during eSWR; CA3 pyramidal cells increased their firing during

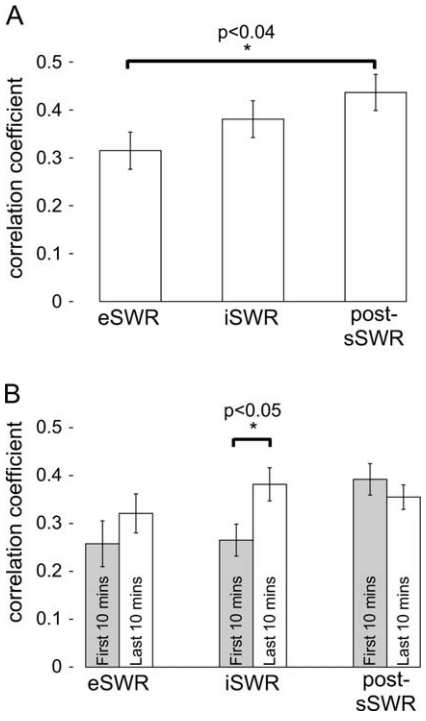


Figure 8. Comparison of Assembly Correlation Coefficients Calculated from the Regression between Theta and e/i/sSWR IFRCs, Measured for the Whole Session, in the Beginning or the End of the Sessions

Waking theta IFRCs were measured for the whole recording, whereas SWR IFRCs were measured for either the whole session (A) or for the first or last 10 min of the corresponding waking or sleep session (B). Regression coefficients were calculated separately for each recording session and averaged (±SE). Number of sessions: (A) eSWR, n = 17; iSWR, n = 19; post-sSWR, n = 18; (B) eSWR, n = 11; iSWR, n = 14; post-sSWR, n = 18. Note the significantly larger correlation for post-sSWR as compared to eSWRs and for iSWRs measured in the last 10 min as compared to the first 10 min of the recorded sessions.

eSWRs in conjunction with negative sharp waves in the CA1 radiatum, indicating that Schaffer collateral synapses are activated (Buzsaki et al., 1983; Ylinen et al., 1995; Csicsvari et al., 1999b). However, the average sharp wave amplitude during eSWRs was lower (30%–60%) than during sleep. Acetylcholine has been shown to suppress excitatory neurotransmission on proximal dendrites of hippocampal pyramidal cells in vitro, through presynaptic muscarinic receptors (Hounsgaard, 1978; Dutar and Nicoll, 1988; Hasselmo and Schnell, 1994; cf. Hasselmo, 1999). During eSWRs, such suppression can explain the reduction of sharp wave amplitudes and is expected to reduce CA1 network responses. Nevertheless, we have observed only a minor reduction in the eSWR network firings; there was only a 10%–15% reduction of pyramidal SWR firing rate and network synchrony relative to sSWRs. However, acetylcholine and other nonspecific subcortical neurotransmitters are known to make pyramidal cells more excitable via their action on postsynaptic receptors (Madison and Nicoll, 1986; Madison et al., 1987; Benardo, 1993), which could compensate for the reduced effectiveness of the CA3 inputs.

Unlike during sSWRs, place-selective firing can facilitate the eSWR-related firing of spatially active place cells. We have shown that location-specific firing remains prior to eSWRs, confirmed by the increased baseline of eSWR firing histograms inside the place field and by the finding that place rate-map similarity reaches baseline (theta) levels within only 100–150 ms from the eSWR peak. This enables inputs that drive place-selective activity and SWR network bursts to summate on CA1 pyramidal dendrites. The increased SWR peak inside the place field and the monotonically increasing eSWR peak-against-baseline function (Figure 5B) indicates that, indeed, such summation can take place.

The SWR peak firing inside the place field was not only stronger than outside the place field but it exceeded the sum of the SWR peak firing outside and the baseline firing differences. This stronger-than-the-sum activation was also confirmed by the >1 first derivative of the eSWR peak-against-baseline function. SWR-firing outside the place field estimates eSWR responses in the absence of place-selective activity; while the increase of the baseline firing rate corresponds to the place-selective increase. Thus, our results suggest that the firing response during eSWRs is stronger than the sum of place-independent eSWR and place-selective firing responses. The supralinear summation of dendritic EPSPs or EPSPs with dendritic action potentials could explain these results (Yuste and Denk, 1995; Magee and Johnston, 1997; Williams and Stuart, 2000; Nettleton and Spain, 2000) because active dendritic spikes have been observed in vivo during SWRs (Kamondi et al., 1998). However, "supralinear" summation of EPSPs itself is not required for such stronger-than-the-sum firing increase; the "linear" summation of two subthreshold EPSPs, together reaching the action potential threshold, could result in a "supralinear" increase of the firing response.

### Assembly Coding of Reactivated Memory Traces

There is increasing evidence that it is not the independent activity of single neurons but their joint firings in ensembles that encodes reactivated memory traces. It has been demonstrated that even some events that occurred during the previous 24 hr are reactivated (Kudrimoti et al., 1999; Hirase et al., 2001), which makes it likely that memory traces of multiple environments recur during sleep. Cooperative neuronal responses may simultaneously encode both the environment and the location within it, which cannot be achieved by individual cells alone. Such cooperativeness among recurring neuronal responses is indicated by the reactivation of waking co-firing patterns during sleep. Furthermore, our result that the co-firing matrix of recorded assemblies is correlated between theta and sSWRs shows that joint firing patterns of recorded neuronal groups recur in sSWRs and thus provides further proof for assembly coding during reactivation.

It has not been fully resolved whether reactivated neuronal patterns represent movement paths or places that the animal visited. To date, most studies have assumed the former, interpreting recurrence of co-firing patterns as reactivation of cells with overlapping place fields that fire across a reactivated movement path. However, recurring firing sequences have been identified only on linear or circular tracks, where similar movement paths are repeated many times (Skaggs and McNaughton, 1996; Louie and Wilson, 2001; Lee and Wilson, 2002, 2004).

We were able to show a weak reactivation of firing sequences during sSWRs, though not in those cell pairs with nearly symmetrical cross-correlations during exploration. Nevertheless, these cell pairs showed a significant reactivation of their co-firing patterns during sSWRs. Therefore, our data indicate that some of the reactivated assembly patterns represent space without being part of a firing sequence representing movement paths.

Reactivated assembly firing patterns may also code for location-independent information. In waking exploration, some of the neuronal and assembly firing patterns are independent of the location of the animal (Wood et al., 1999; Harris et al., 2003; Huxter et al., 2003). Place cells also fire outside their place field during eSWRs, indicating that eSWR firing may have a location-independent component. Furthermore, such location-independent firing eSWR patterns may be reactivated during sSWRs, suggested by the stronger correlation between IFRCs (theta versus post-sSWR) than between place field similarity and post-sSWR IFRC.

### Neuronal Plasticity underlying Reactivation

Although STDP may contribute to the reactivation assemblies that fire in sequences (Skaggs et al., 1996; Mehta et al., 2000, 2002; Ekstrom et al., 2001), it cannot explain the reactivated co-firing patterns for cells that do not follow such sequences. We have confirmed that cell pairs that did not show sequential firing bias still showed reactivation of their co-firing patterns (i.e., cell that may encode location but not movement paths per se). Therefore, the sequential activation of place cells, which would enable STDP, is not required for the reactivation of waking co-firing patterns, and some other form of plasticity may be required for the reactivation co-firing patterns that may encode location without encoding movement paths.

We propose that eSWRs may facilitate the formation of place-related assemblies that are reactivated during sleep through facilitating connections between place cells with similar place fields. Such facilitation can also explain the reactivation of co-firing patterns. The firing of CA1 pyramidal cells is potentiated during SWRs (even in behaving animals) following SWR-paired cell stimulation (King et al., 1999). During eSWRs, a similar pairing can be provided by the overlap of place-selective firing with eSWR network bursts, which we observed. Therefore, it is expected that CA1 pyramidal cells that fire together during eSWRs will have potentiated connections with the same presynaptic CA3 cell groups. Furthermore, by showing the place-selective firing of CA3 pyramidal cells during eSWRs, we confirmed that both CA3 and CA1 place cells with similar place fields can fire together during eSWRs. Thus, the coupling of place-related activity with eSWRs is expected to result in the potentiation of synaptic weights of CA3 and CA1 cells with similar place cells, consequently enabling these cells to fire together during subsequent i/sSWRs.

By monitoring changes in the co-firing assembly patterns during iSWRs (that are not directly driven by place-selective firing), we tested to what degree waking co-firing patterns are incorporated into exiting SWR patterns during the course of exploration. The regression coefficient of theta-iSWR IFRCs was significantly higher toward the end of the session, suggesting that waking patterns are incorporated into existing SWR patterns gradually during the course of exploration. We have not detected similar changes for post-sSWR patterns, suggesting that changes in SWR ensemble representations primarily occur during exploration.

Additional support for a role of eSWRs in plasticity comes from the study of Jarosiewicz and Skaggs, 2004, showing that place cells that fire at the location where the animal fell asleep are frequently reactivated in sleep. eSWRs occur frequently at the sleep location as the animal settles down, which may ensure plastic changes so these cells can be reactivated strongly in sleep even outside SWRs. However, eSWR may not occur in sufficient numbers to cover all possible reactivated assembly patterns; other network-burst patterns such as 110 Hz "small ripples" (Csicsvari et al., 1999b, 2000) or gamma-burst patterns (Leung, 1979; Buzsaki et al., 1983; Bragin et al., 1995; Csicsvari et al., 2003) that occur more frequently may have a similar role. Further work is required to unveil the details of how SWRs and other network-burst patterns may be involved in plastic processes. Increasing availability of in vitro models of fast-oscillatory patterns may help to further address these questions (Draguhn et al., 1998; Fisahn et al., 1998; Maier et al., 2003; Colgin et al., 2004; Nimmrich et al., 2005; Mann et al., 2005).

Overall, coupling of behaviorally driven activity (i.e., spatial firing) with a network burst pattern (i.e., eSWRs) may be one mechanism by which behaviorally driven neuronal activity patterns are stored and associated neuronal assemblies formed through synaptic modification.

## Experimental Procedures

### Surgery and Recordings

Six male rats (four Long Evans and two Hooded Lister strains; 3–8 months, 300–500 g) and one additional young male Sprague-Dawley rat (2.5 months, 350 g) were implanted with four to eight independently movable wire tetrodes under deep anesthesia using isoflurane (0.5%–3%), oxygen (1–2 l/min), and an initial dose of buprenorphine (0.1 mg/kg). Tetrodes (M.L. Recce and J. O'Keefe, 1989, Soc. Neurosci., abstract) were attached to the microdrives, enabling their independent movement. The tetrodes were constructed from four individual tungsten wires, 12 μm in diameter (H-Formvar insulation with Butyral bond coat, California Fine Wire, Grover Beach, CA), twisted and then heated in order to bind them into a single bundle. The tips were then gold plated to reduce their electrode impedance to 200–600 kΩ. During surgery, a craniotomy was performed above the dorsal hippocampus, centered at AP = −3.8; ML = 2.5, and the dura mater was removed. The electrode bundles were then implanted into the superficial layers of the neocortex, after which both the exposed cortex and electrode shanks were sealed with paraffin wax. Two 50 μm single tungsten wires (California Fine Wire) with 2 mm of the insulation removed were inserted into the cerebellum or attached to screws above the cerebellum and served as ground and reference electrodes. To permanently attach the drive assembly to the scull, six to ten additional stainless-steel anchor screws were used. The paraffin wax-coated electrodes and microdrives were then daubed with dental acrylic to encase the electrode-microdrive assembly and anchor it to the screws in the scull.

Following a recovery period of 7 days, the tetrodes were lowered into the CA1 region of the hippocampus, over a further period of up to 7 days. A 32 channel unity-gain preamplifier panel (http://www.braintelemeter.atw.hu) was used to reduce cable-movement artifacts.

Wide-band (0.1/1 Hz to 5 kHz) recordings were taken, and the amplified local field potential (×1000, via a 64 channel Sensorium Amplifier, Charlotte, VT) and multiple-unit activity were continuously

digitized at 20 kHz using a 64 channel AD converter computer card (United Electronics Industries, Canton, MA). Small infrared light-emitting diodes mounted on the headstage were used to track the location of the animal.

The animals were housed in a separate room and were taken to the recording room prior to the experiments. Food and water were freely available for the animal prior to the recording procedures. Recordings were always performed in the same room. The recording apparatus that was used consisted of various environments in various locations within the recording environment, including rectangular boxes of different sizes (20–50cm width) and material (plastic, wooden, or paper) and, occasionally, simple maze configurations. Black wooden walls (50 cm height) always closely surrounded the environment, and recordings were always performed in darkness. This limited the animals' access to distal room cues during the recordings, and no local cues such as cue cards were used in the experiments. Each recording session consisted of pre-sleep (in a different environment from that used for exploration), waking spatial exploration, and post-sleep periods. Sleep sessions were at least 20 min long, whereas the length of waking session was varied according to the time required for the animal to fall asleep. Nevertheless, for at least 20 min the animal was not allowed to settle down to sleep and was encouraged to explore the environment, as needed, using appetitive food reward (chocolate sprinkles). The location of the animal was constantly monitored even during sleep periods. Following the post-sleep period, the animal was placed in a different environment for exploration and subsequent sleep. Sleep in the previous environment provided pre-sleep for this new session. Depending on the willingness of the animal, typically one to two complete [pre-sleep]-exploration-[post-sleep] sessions were recorded in a day.

After completion of the experiments, the rats were deeply anesthetized and perfused through the heart, first with 0.9% saline solution followed by a 4% buffered formalin phosphate solution for the histological verification of the electrode tracks.

All procedures involving experimental animals were carried out in accordance with the Animals (Scientific Procedures) Act, 1986 (UK) and associated procedures under an approved project license.

### Data Analysis

Unit isolation and clustering procedures have been described before (Csicsvari et al., 1998). Briefly, action potentials were extracted from the digitally high-pass filtered (0.8–5 kHz) signal. The power computed in a sliding window (12.8 ms) and action potentials with a power of >5 SD from the baseline mean were selected. The spike features were then extracted by using principal components analyses. The detected action potentials were then segregated into putative multiple single units by using automatic clustering software (Harris et al., 2001, http://klustakwik.sourceforge.net/). Finally, the generated clusters were manually refined by a graphical cluster cutting program (Csicsvari et al., 1998). Only units with clear refractory periods in their autocorrelation and well-defined cluster boundaries (Harris et al., 2001) were used for further analysis. Pyramidal cells and interneurons were discriminated by their autocorrelations, firing rate, and wave forms, as previously described (Csicsvari et al., 1999a). Periods of waking spatial exploration, immobility, and sleep were clustered together. Stability of the cells was verified by plotting spike features over time and by plotting two-dimensional unit cluster plots in different sessions (Figure S3). In addition, an isolation distance (based on Mahabalonis distance, Harris et al., 2001) is calculated to ensure that the spike clusters do not overlap during the course of the recordings.

Both theta detection (Csicsvari et al., 1998) and SPW detection (Csicsvari et al., 1998, 1999a) were performed as previously described. To identify periods of theta activity, the theta/delta power ratio was measured in 1600 ms segments (800 ms steps in between measurement windows), using Thomson's multi-taper method (Thomson, 1982; Mitra and Pesaran, 1999). Exploratory epochs included periods of locomotion or the presence of theta oscillations (as seen in the theta/delta ratio), including a <2.4 s (i.e., two consecutive windows) transient from immobility segments. Waking immobility sessions were selected when both the speed and theta-delta ratio were below a preset threshold for at least 2.4 s interval. Sleep sessions were recorded separately and were identified by occasional occurrence of REM-theta periods and the presence of slow wave oscillations.

For the detection of theta-oscillatory waves, local field potential was filtered (5–28 Hz), and the negative peaks of individual theta waves were then detected. For the detection of SWRs, local field potentials were band-pass filtered (150–250 Hz), and a reference signal (from a channel that did not contain ripple oscillations) was subtracted to eliminate common-mode noise (such as muscle artifacts). The power (root mean square) of the filtered signal was calculated for each electrode and summed across electrodes designated as being in the CA1 pyramidal cell layer. The threshold for SWR detection was set to 7 standard deviations (SD) above the background mean. The SWR detection threshold was always set in the first available sleep session, and the same threshold was used for all other sessions.

For the calculation of cross-correlation histograms, 1 ms bins were used. Histograms with less than 50 joint unit-discharges were excluded from averaging to avoid the bias of sparse histograms. Note that this analysis overestimated the average correlation strength of nonoverlapping cell pairs in eSWRs because, in most of the cases, they fired together rarely and many of them were excluded to avoid the bias of sparse histograms. Note that cross-correlations were always performed between units recorded in different electrodes only and, during clustering, we paid special attention not to split bursting pyramidal cells into multiple cell clusters that, cumulatively, may cause cross-correlation asymmetry, even between units on different electrodes (Quirk and Wilson, 1999).

To measure the IFRCs, spike counts were measured in 50 ms windows, which were SWR peak-centered for SWR periods and consecutive windows for theta epochs. Only those sessions with more than 100 detected SWRs were selected. Only those correlations were considered in which both cells fired at least 50 times in the measurement time windows and where the cells were detected from a different electrode. Place rate-maps were calculated as described before (Harris et al., 2001) by a kernel-based method in which both the firing rate and occupancy maps were smoothed with a Gaussian kernel function (SD = 3 cm). Pearson correlation coefficient of the place rate-maps was calculated to compare place fields.

### Supplemental Data

The Supplemental Data for this article can be found online at http://www.neuron.org/cgi/content/full/49/1/143/DC1/.

### Acknowledgments

We thank G. Buzsaki, M. Capogna, A. Czurko, J. Huxter, T. Klausberger, X. Leinekugel, P. Magill, O. Paulsen, I. Szabo, and the anonymous reviewers for their constructive comments on the manuscript; and N. Campo-Urriza for the technical assistance. This work was supported by the Medical Research Council, UK. T. Senior's D.Phil. studentship is funded by the Wellcome Trust, UK.

Received: March 29, 2005
Revised: June 29, 2005
Accepted: October 18, 2005
Published: January 4, 2006

### References

Benardo, L.S. (1993). Characterization of cholinergic and noradrenergic slow excitatory postsynaptic potentials from rat cerebral cortical neurons. Neuroscience *53*, 11–22.

Bi, G.Q., and Poo, M.M. (1998). Synaptic modifications in cultured hippocampal neurons: dependence on spike timing, synaptic strength, and postsynaptic cell type. J. Neurosci. *18*, 10464–10472.

Bragin, A., Jando, G., Nadasdy, Z., Hetke, J., Wise, K., and Buzsaki, G. (1995). Gamma (40–100 Hz) oscillation in the hippocampus of the behaving rat. J. Neurosci. *15*, 47–60.

Buzsaki, G. (1986). Hippocampal sharp waves: their origin and significance. Brain Res. *398*, 242–252.

Buzsaki, G. (1989). Two-stage model of memory trace formation: a role for "noisy" brain states. Neuroscience *31*, 551–570.

Buzsaki, G. (1996). The hippocampo-neocortical dialogue. Cereb. Cortex *6*, 81–92.

Buzsaki, G. (2002). Theta oscillations in the hippocampus. Neuron *33*, 325–340.

Buzsaki, G., Leung, L.W., and Vanderwolf, C.H. (1983). Cellular bases of hippocampal EEG in the behaving rat. Brain Res. *287*, 139–171.

Buzsaki, G., Horvath, Z., Urioste, R., Hetke, J., and Wise, K. (1992). High-frequency network oscillation in the hippocampus. Science *256*, 1025–1027.

Colgin, L.L., Kubota, D., Jia, Y., Rex, C.S., and Lynch, G. (2004). Long-term potentiation is impaired in rat hippocampal slices that produce spontaneous sharp waves. J. Physiol. *558*, 953–961.

Csicsvari, J., Hirase, H., Czurko, A., and Buzsaki, G. (1998). Reliability and state dependence of pyramidal cell-interneuron synapses in the hippocampus: an ensemble approach in the behaving rat. Neuron *21*, 179–189.

Csicsvari, J., Hirase, H., Czurko, A., Mamiya, A., and Buzsaki, G. (1999a). Oscillatory coupling of hippocampal pyramidal cells and interneurons in the behaving Rat. J. Neurosci. *19*, 274–287.

Csicsvari, J., Hirase, H., Czurko, A., Mamiya, A., and Buzsaki, G. (1999b). Fast network oscillations in the hippocampal CA1 region of the behaving rat. J. Neurosci. *19*, RC20.

Csicsvari, J., Hirase, H., Mamiya, A., and Buzsaki, G. (2000). Ensemble patterns of hippocampal CA3–CA1 neurons during sharp wave-associated population events. Neuron *28*, 585–594.

Csicsvari, J., Jamieson, B., Wise, K.D., and Buzsaki, G. (2003). Mechanisms of gamma oscillations in the hippocampus of the behaving rat. Neuron *37*, 311–322.

Czurko, A., Hirase, H., Csicsvari, J., and Buzsaki, G. (1999). Sustained activation of hippocampal pyramidal cells by 'space clamping' in a running wheel. Eur. J. Neurosci. *11*, 344–352.

Draguhn, A., Traub, R.D., Schmitz, D., and Jefferys, J.G. (1998). Electrical coupling underlies high-frequency oscillations in the hippocampus in vitro. Nature *394*, 189–192.

Dutar, P., and Nicoll, R.A. (1988). Classification of muscarinic responses in hippocampus in terms of receptor subtypes and second-messenger systems: electrophysiological studies in vitro. J. Neurosci. *8*, 4214–4224.

Ekstrom, A.D., Meltzer, J., McNaughton, B.L., and Barnes, C.A. (2001). NMDA receptor antagonism blocks experience-dependent expansion of hippocampal "place fields". Neuron *31*, 631–638.

Fisahn, A., Pike, F.G., Buhl, E.H., and Paulsen, O. (1998). Cholinergic induction of network oscillations at 40 Hz in the hippocampus in vitro. Nature *394*, 186–189.

Harris, K.D., Hirase, H., Leinekugel, X., Henze, D.A., and Buzsaki, G. (2001). Temporal interaction between single spikes and complex spike bursts in hippocampal pyramidal cells. Neuron *32*, 141–149.

Harris, K.D., Csicsvari, J., Hirase, H., Dragoi, G., and Buzsaki, G. (2003). Organization of cell assemblies in the hippocampus. Nature *424*, 552–556.

Hasselmo, M.E. (1999). Neuromodulation: acetylcholine and memory consolidation. Trends Cogn. Sci. *3*, 351–359.

Hasselmo, M.E., and Schnell, E. (1994). Laminar selectivity of the cholinergic suppression of synaptic transmission in rat hippocampal region CA1: computational modeling and brain slice physiology. J. Neurosci. *14*, 3898–3914.

Hirase, H., Leinekugel, X., Czurko, A., Csicsvari, J., and Buzsaki, G. (2001). Firing rates of hippocampal neurons are preserved during subsequent sleep episodes and modified by novel awake experience. Proc. Natl. Acad. Sci. USA *98*, 9386–9390.

Hounsgaard, J. (1978). Presynaptic inhibitory action of acetylcholine in area CA1 of the hippocampus. Exp. Neurol. *62*, 787–797.

Huxter, J., Burgess, N., and O'Keefe, J. (2003). Independent rate and temporal coding in hippocampal pyramidal cells. Nature *425*, 828–832.

Jarosiewicz, B., and Skaggs, W.E. (2004). Hippocampal place cells are not controlled by visual input during the small irregular activity state in the rat. J. Neurosci. *24*, 5070–5077.

Kamondi, A., Acsady, L., and Buzsaki, G. (1998). Dendritic spikes are enhanced by cooperative network activity in the intact hippocampus. J. Neurosci. *18*, 3919–3928.

King, C., Henze, D.A., Leinekugel, X., and Buzsaki, G. (1999). Hebbian modification of a hippocampal population pattern in the rat. J. Physiol. *521*, 159–167.

Kudrimoti, H.S., Barnes, C.A., and McNaughton, B.L. (1999). Reactivation of hippocampal cell assemblies: effects of behavioral state, experience, and EEG dynamics. J. Neurosci. *19*, 4090–4101.

Lee, A.K., and Wilson, M.A. (2002). Memory of sequential experience in the hippocampus during slow wave sleep. Neuron *36*, 1183–1194.

Lee, A.K., and Wilson, M.A. (2004). A combinatorial method for analyzing sequential firing patterns involving an arbitrary number of neurons based on relative time order. J. Neurophysiol. *92*, 2555–2573.

Leung, S.W. (1979). Potentials evoked by alvear tract in hippocampal CA1 region of rats. II. Spatial field analysis. J. Neurophysiol. *42*, 1571–1589.

Louie, K., and Wilson, M.A. (2001). Temporally structured replay of awake hippocampal ensemble activity during rapid eye movement sleep. Neuron *29*, 145–156.

Madison, D.V., and Nicoll, R.A. (1986). Actions of noradrenaline recorded intracellularly in rat hippocampal CA1 pyramidal neurones, in vitro. J. Physiol. *372*, 221–244.

Madison, D.V., Lancaster, B., and Nicoll, R.A. (1987). Voltage clamp analysis of cholinergic action in the hippocampus. J. Neurosci. *7*, 733–741.

Magee, J.C., and Johnston, D. (1997). A synaptically controlled, associative signal for Hebbian plasticity in hippocampal neurons. Science *275*, 209–213.

Maier, N., Nimmrich, V., and Draguhn, A. (2003). Cellular and network mechanisms underlying spontaneous sharp wave-ripple complexes in mouse hippocampal slices. J. Physiol. *550*, 873–887.

Mann, E.O., Suckling, J.M., Hajos, N., Greenfield, S.A., and Paulsen, O. (2005). Perisomatic feedback inhibition underlies cholinergically induced fast network oscillations in the rat hippocampus in vitro. Neuron *45*, 105–117.

Markram, H., Lubke, J., Frotscher, M., and Sakmann, B. (1997). Regulation of synaptic efficacy by coincidence of postsynaptic APs and EPSPs. Science *275*, 213–215.

Mehta, M.R., Quirk, M.C., and Wilson, M.A. (2000). Experience-dependent asymmetric shape of hippocampal receptive fields. Neuron *25*, 707–715.

Mehta, M.R., Lee, A.K., and Wilson, M.A. (2002). Role of experience and oscillations in transforming a rate code into a temporal code. Nature *417*, 741–746.

Mitra, P.P., and Pesaran, B. (1999). Analysis of dynamic brain imaging data. Biophys. J. *76*, 691–708.

Nadasdy, Z., Hirase, H., Czurko, A., Csicsvari, J., and Buzsaki, G. (1999). Replay and time compression of recurring spike sequences in the hippocampus. J. Neurosci. *19*, 9497–9507.

Nettleton, J.S., and Spain, W.J. (2000). Linear to supralinear summation of AMPA-mediated EPSPs in neocortical pyramidal neurons. J. Neurophysiol. *83*, 3310–3322.

Nimmrich, V., Maier, N., Schmitz, D., and Draguhn, A. (2005). Induced sharp wave-ripple complexes in the absence of synaptic inhibition. J. Physiol. *563*, 663–670.

O'Keefe, J., and Dostrovsky, J. (1971). The hippocampus as a spatial map. Preliminary evidence from unit activity in the freely-moving rat. Brain Res. *34*, 171–175.

O'Keefe, J., and Nadel, L. (1978). Hippocampus as a Cognitive Map (Oxford: Clarindon).

Quirk, M.C., and Wilson, M.A. (1999). Interaction between spike waveform classification and temporal sequence detection. J. Neurosci. Methods *94*, 41–52.

Skaggs, W.E., and McNaughton, B.L. (1996). Replay of neuronal firing sequences in rat hippocampus during sleep following spatial experience. Science *271*, 1870–1873.

Skaggs, W.E., McNaughton, B.L., Wilson, M.A., and Barnes, C.A. (1996). Theta phase precession in hippocampal neuronal populations and the compression of temporal sequences. Hippocampus *6*, 149–172.

Squire, L.R., and Zola-Morgan, S. (1991). The medial temporal lobe memory system. Science *253*, 1380–1386.

Suzuki, S.S., and Smith, G.K. (1988). Spontaneous EEG spikes in the normal hippocampus. II. Relations to synchronous burst discharges. Electroencephalogr. Clin. Neurophysiol. *69*, 532–540.

Thomson, D.J. (1982). Spectrum estimation and harmonic analysis. Proc. IEEE *70*, 1055–1096.

Traub, R.D., and Bibbig, A. (2000). A model of high-frequency ripples in the hippocampus based on synaptic coupling plus axon-axon gap junctions between pyramidal neurons. J. Neurosci. *20*, 2086–2093.

Vanderwolf, C.H. (1969). Hippocampal electrical activity and voluntary movement in the rat. Electroencephalogr. Clin. Neurophysiol. *26*, 407–418.

Williams, S.R., and Stuart, G.J. (2000). Backpropagation of physiological spike trains in neocortical pyramidal neurons: implications for temporal coding in dendrites. J. Neurosci. *20*, 8238–8246.

Wilson, M.A., and McNaughton, B.L. (1994). Reactivation of hippocampal ensemble memories during sleep. Science *265*, 676–679.

Wood, E.R., Dudchenko, P.A., and Eichenbaum, H. (1999). The global record of memory in hippocampal neuronal activity. Nature *397*, 613–616.

Ylinen, A., Bragin, A., Nadasdy, Z., Jando, G., Szabo, I., Sik, A., and Buzsaki, G. (1995). Sharp wave-associated high-frequency oscillation (200 Hz) in the intact hippocampus: network and intracellular mechanisms. J. Neurosci. *15*, 30–46.

Yuste, R., and Denk, W. (1995). Dendritic spines as basic functional units of neuronal integration. Nature *375*, 682–684.